EPSC Abstracts
Vol. 16, EPSC2022-562, 2022, updated on 18 Oct 2022
https://doi.org/10.5194/epsc2022-562
Europlanet Science Congress 2022

Comparing Methods for Gravitational Computation: Studying the Effect of Inhomogeneities

Matthias Noeker[1,2,5], Hermann Meißenhelter[3,5], Tom Andert[4], René Weller[3], Özgür Karatekin[1], and Benjamin Haser[4]

[1]Royal Observatory of Belgium, Brussels, Belgium (matthias.noeker@observatory.be).
[2]Université catholique de Louvain, Ottignies-Louvain-la-Neuve, Belgium
[3]Institute for Computer Graphics and Virtual Reality University of Bremen, Bremen, Germany
[4]Institute of Space Technology and Space Applications (ISTA), Bundeswehr University, Munich, Germany
[5]These authors contributed equally.

Introduction

Current and future small body missions, such as the ESA Hera mission [1] or the JAXA MMX mission [2] demand good knowledge of the gravitational field of the targeted celestial bodies. This is not only motivated to ensure the precise spacecraft operations around the body, but likewise important for landing manoeuvres, surface (rover) operations, and science, including surface gravimetry [3]. To model the gravitation of irregularly-shaped, non-spherical bodies, different methods exist. Previous work performed a comparison between three different methods [4], considering a homogeneous density distribution inside the body. In this work, the comparison is continued, by introducing a first inhomogeneity inside the body. For this, the same three methods, being the polyhedral method [5] and two different mascon methods [6][7] are compared. We will describe the methods and our test cases in the next Section.

Methodology

The polyhedral method (PM) provides an analytical solution to the gravitational potential field of any polyhedral body [5]. Intrinsically, the method demands a homogeneous density throughout the body, making it not directly applicable to account for inhomogeneities. Therefore, in this work, we perform a superposition of the gravitational fields of the main body and the inhomogeneities, considering the *differential* density, which can also be negative.

The other two methods are based on mascons, namely MSP (Mascons: Sphere Packing) and MASC (Mascons: Spherical Coordinates). These mascon methods subdivide a body into smaller parts. The mass is then concentrated in the centre of these parts and the gravitational field is the sum of the individual accelerations. MSP uses a sphere packing with non-uniform-sized spheres that do not overlap (see Fig.1). Since the sphere packing does not cover the complete volume, we use additionally a heuristic that tends to assign smaller spheres more mass. To model inhomogeneity, we compute separate sphere packings with different densities assumed. With MASC, the internal mass distribution is modelled by dividing the body in longitude, latitude, and radius, and by assigning individual densities to the resulting set of tesseroids.

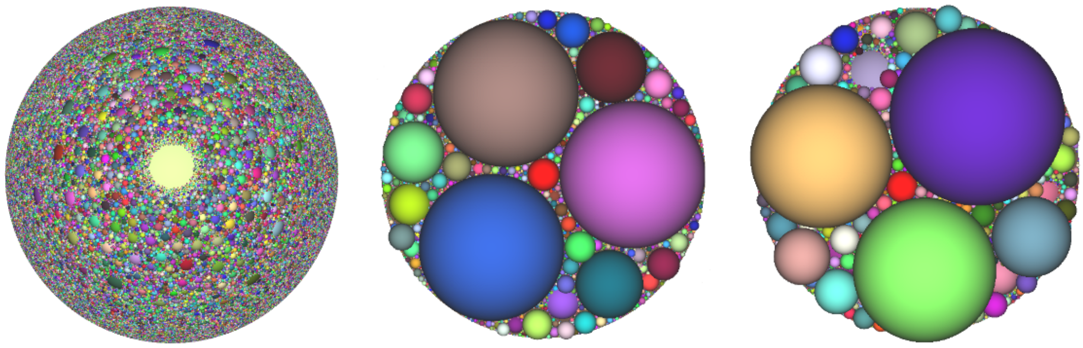

(a) Sphere packing with 800k spheres.

(b) Cross-section with red core at center $\vec{p} = (0, 0, 0)$.

(c) Cross-section with red core at position $\vec{p} = (-100, -100, 0)$.

Figure 1: Sphere packings created and used by the MSP approach are shown. a) complete packing for case I. b) and c) the packing cross-sections for the two investigated cases (I, II).

Test Cases

Our two test cases consider two nested ideal spheres that are approximated through a UV-Sphere with 328,328 facets [4]. The outer sphere has a radius r=1,000 m and a density of 1.0g/cm^3, and the inner sphere has a radius r=100 m and a density of 0.5g/cm^3. In Case I, the inner sphere is placed concentric to the outer sphere, whereas in Case II the sphere's centre is translated to X=−100 m and Y=−100 m. We compute the gravitational acceleration for points on the ideal sphere and compare it to the analytical solution through a relative error. Clearly, the ratio of computed and analytical solution $\tau = g_{com} / g_{ana}$ should always be <100% as the UV-sphere is only an approximation of the perfect sphere, values >100% represent an overshoot. This agreement ratio is presented in the next Section.

First Results

The overall results and range of τ on the surface of the sphere are summarized in Table 1:

Table 1: Comparison of all methods with the analytic solution. Case (I) is the core at center, and case (II) is the moved core. The number in the name indicates the number of mascons. Gravitational constant used: $6.674 \times 10^{-11}\,\mathrm{m^3\,kg^{-1}\,s^{-2}}$.

Case	**Method**	**Min. [%]**	**Mean [%]**	**Max. [%]**	σ [%]
I	PM	99.993143	99.995461	99.997864	0.000942
	MSP 800k	99.542132	99.996047	100.345711	0.117449
	MASC 64.8k	99.994138	99.995459	100.004137	0.001201
II	PM	99.993143	99.995461	99.997864	0.000942
	MSP 800k	99.590773	99.995998	100.307859	0.111008
	MASC 64.8k	99.994137	99.995459	100.004158	0.001201

For both of our cases, PM delivers the most accurate results (Table 1). The error results from the shape approximation. It is visualized in Figures 1 and 2. We can see the expected shift from an almost equal to an unequal surface gravity. In Figure 1 we can also see that the shape approximation error is larger than the floating-point precision limitation (noisy pattern, Figure 1a).

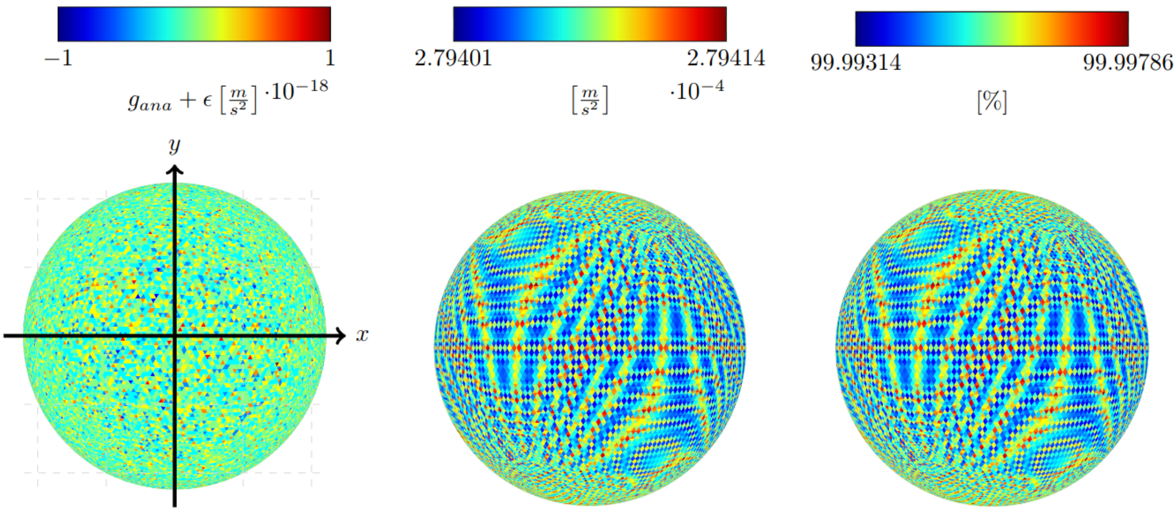

(a) Analytic solution.

(b) Solution with polyhedral method.

(c) Relative error between solutions.

Figure 2: Comparison of the surface gravity between the analytic solution g_{ana} and polyhedral method with the core at the center $\vec{p} = (0, 0, 0)$. Core density is $0.5\,\mathrm{g/cm^3}$ and outer density is $1.0\,\mathrm{g/cm^3}$.

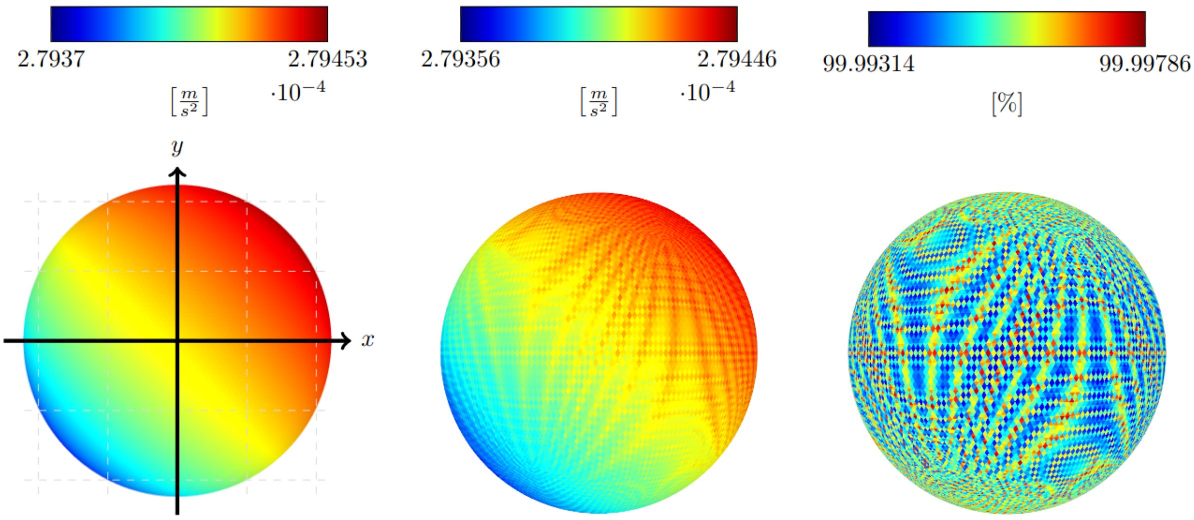

(a) Analytic solution.

(b) Solution with polyhedral method.

(c) Relative error between solutions.

Figure 3: Comparison of the surface gravity between the analytic solution and polyhedral method with the moved core from center $\vec{p} = (-100, -100, 0)$. Core density is $0.5\,\mathrm{g/cm^3}$ and outer density is $1.0\,\mathrm{g/cm^3}$.

The MSP method creates a noisy overshooting pattern (see Figures 4b and 4c), which results from the spheres near the surface and the heuristic. Large spheres lead to a circular artifact at the surface. Observable at the center of Figures 4b and 1a. It is a similar pattern for Case II. The MASC error results from the subdivision in spherical coordinates. At the poles the number of tesseroids increases, which leads to a circular overshoot at two sides. It is also true for the shifted core (see Figure 4a). The computation time for MSP remained the same as for the homogeneous case [4] while it has doubled for PM and MASC.

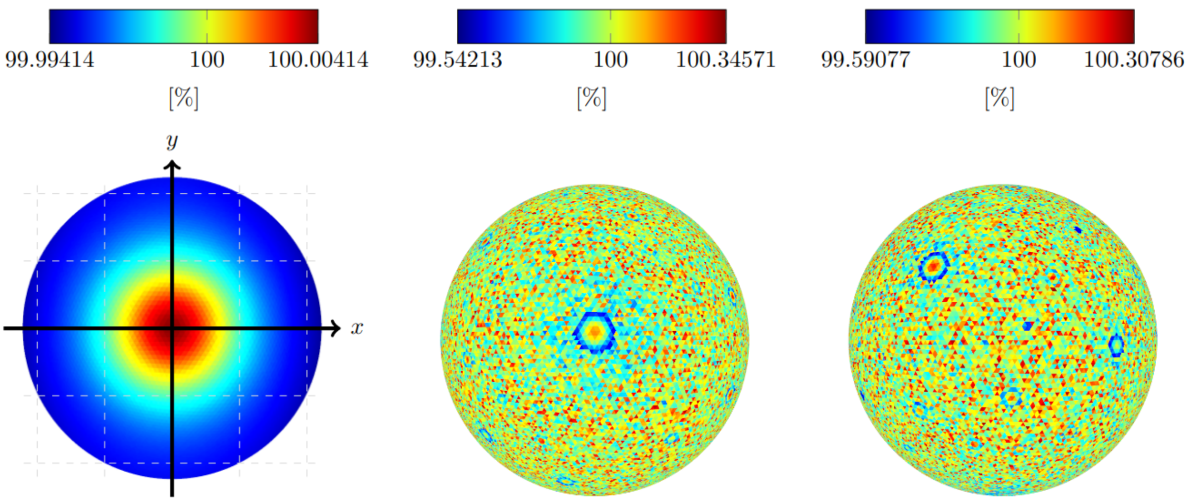

(a) MASC with core at center.

(b) MSP with core at center.

(c) MSP with moved core.

Figure 4: Relative error between the analytic solutions and the mascon methods (MASC, MSP). Note: The visual error for MASC is practically identical for both cases.

The three methods presented above for the computation of the gravitational acceleration will be applied to more complex shapes for irregularly shaped bodies. In addition, different inhomogeneous density distributions representing the interior will be studied and the according results presented.

Acknowledgements

M.N. acknowledges funding from the Foundation of German Business (sdw) and the Royal Observatory of Belgium (ROB) PhD grants. The work by Bundeswehr University was carried out in the frame of project KaNaRiA-NaKoRa which is funded by DLR under grant FKZ50NA1915. The work on the part of University of Bremen presented in this paper was partially funded by DLR under grant 50NA1916.

References

[1] Michel, Patrick, et al. "The Hera mission: European component of the ESA-NASA AIDA mission to a binary asteroid." 42nd COSPAR Scientific Assembly 42 (2018):B1-1.

[2] Campagnola, Stefano, et al. "Mission analysis for the Martian Moons Explorer (MMX) mission." Acta Astronautica 146 (2018):409-417.

[3] Noeker, Matthias, et al. "The GRASS Gravimeter Rotation Mechanism for ESA Hera Mission On-Board Juventas Deep Space CubeSat." Proceedings of the 46th Aerospace Mechanisms Symposium, Virtual, May 11-13, (2022):159-172.

[4] Meißenhelter, Hermann, et al. "Efficient and Accurate Methods for Computing the Gravitational Field of Irregular-Shaped Bodies." 2022 IEEE Aerospace Conference. IEEE, 2022.

[5] Werner and Scheeres. "Exterior gravitation of a polyhedron derived and compared with harmonic and mascon gravitation representations of asteroid 4769 Castalia." Celestial Mechanics and Dynamical Astronomy 65.3 (1996):313-344.

[6] A. Srinivas, et. al. "Fast and accurate simulation of gravitational field of irregular-shaped bodies using polydisperse sphere packings." in ICAT-EGVE, 2017, pp.213–220.

[7] M. Pätzold, et. al. "Phobos mass determination from the very close flyby of Mars Express in 2010," Icarus, vol. 229, pp. 92–98, Feb.2014.